Hydrogen-bond formation in sodium and potassium hydrosulfides at high pressure

Julian Haines and Andrew G. Christy
Department of Chemistry, University of Leicester, Leicester LE1 7RH, England
(Received 10 April 1992)

Sodium and potassium hydrosulfide were investigated at high pressure using a combination of infrared and Raman spectroscopy and energy dispersive x-ray powder diffraction. NaSH was found to undergo an ordering transition below 9 kbar to yield a cell equivalent to that of the low-temperature phase, but reduced in size. A hydrogen-bonded phase was formed above 83 kbar, the diffraction pattern of which could be fitted using a TlI-type structural model. The refined cell parameters at 130 kbar are $a=7.362(60)$ Å, $b=3.698(38)$ Å, $c=5.615(50)$ Å, $\beta=104.50(51)°$, $Z=4$. The space group would be $P2_1/a$ with bifurcated hydrogen-bonded chains running along **b**. KSH underwent two transitions on compression at 19 and 23 kbar, respectively. The first transition involved only a small volume change. The diffraction data for this phase could be indexed based on a TlI-type model structure, resulting in the following cell at 20 kbar: $a=9.129(41)$ Å, $b=4.181(18)$ Å, $c=6.781(18)$ Å, $\beta=106.47(27)°$, $Z=4$. A large decrease in frequency, increase in bandwidth, and strongly negative $d\nu/dp$ values for the infrared and Raman active S-H stretching vibrations indicated that strong hydrogen bonds were formed at the 23-kbar transition. A unit cell was obtained from the x-ray powder data with $a=7.448(22)$ Å, $b=7.328(26)$ Å, $c=8.110(22)$ Å, $\beta=97.46(36)°$, $Z=8$ at 31 kbar. A structure model with a distorted CsCl structure, related to the hydrogen-bonded, low-temperature phase of CsSD containing four-membered, hydrogen-bonded $S_4D_4^{4-}$ units, is proposed. These and other recently reported results indicate that TlI-type structures are more common than previously believed and are, in fact, the favored intermediates between the NaCl- and CsCl-based structures for systems with nonspherical atoms or ions.

I. INTRODUCTION

The alkali-metal hydroxides and deuteroxides, with the exceptions of LiOH, LiOD, and NaOH, have been shown to undergo transitions at low temperatures to form phases that are characterized by the presence of hydrogen-bonded chains.[1] Among the alkali-metal hydrosulfides and deuterosulfides, only CsSH and CsSD form hydrogen-bonded phases at low temperatures.[2] We have shown that some of the hydroxides and hydrosulfides that do not form hydrogen-bonded phases at low temperatures do form such phases at high pressure, in particular, LiOH,[3] LiOD,[4,5] $LiOH\cdot H_2O$,[6] and the hydrosulfides, NaSH and KSH, discussed herein.

Under ambient conditions, both NaSH and KSH adopt a distorted NaCl structure ($R\bar{3}m$, $Z=3$) with twofold proton disorder,[7,8] Fig. 1. NMR and neutron-scattering studies[9–12] indicated that the SH^- ions perform 180° jumps between the two positions. The cell constants for NaSH (Ref. 11) and KSH (Ref. 8) under ambient conditions are $a=4.463$ Å, $c=9.123$ Å and $a=4.957$ Å, $c=9.916$ Å, respectively. In addition, high-temperature, disordered NaCl-type phases (space group, $Fm3m$, $Z=4$) and low-temperature ordered phases (space group $P2/m$, $Z=2$) exist.[7] These phases have been labeled from the melting point down as phases I, II, and III.

II. EXPERIMENTAL DETAILS

NaSH and KSH (Strem Inc. and Johnson Matthey, Alfa Products) were used without further purification. For the Raman and infrared experiments, the compounds were loaded into the diamond anvil cell (DAC) under a dry nitrogen atmosphere along with a ruby chip as a pressure calibrant.[13] Preindented stainless-steel gaskets of varying thicknesses with initial hole diameters of between 100 and 350 μm were used to contain the sample and calibrant. Nujol was used as a pressure transmitting fluid.

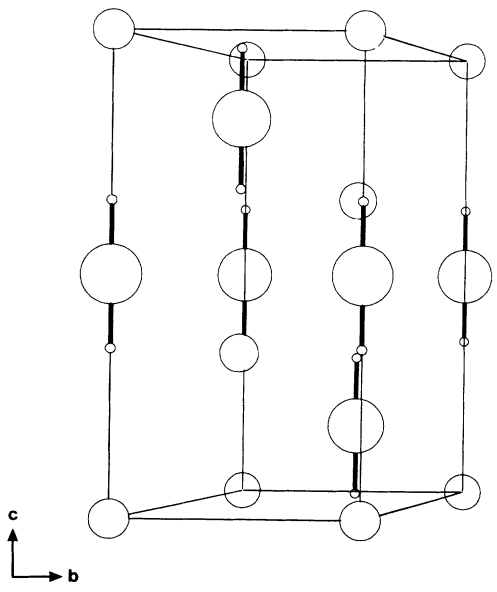

FIG. 1. The structure of ASH (A=Na, K) under ambient conditions: circles represent S (large), A (medium), and 1/2H (small).

Raman spectra were obtained in a back-scattering configuration on a Coderg T800 spectrometer using a Spectra Physics Model 164 argon-ion laser (488.0-nm line) for excitation. Infrared spectra were acquired on a Bio-Rad Digilab FTS-40 spectrometer.

Energy-dispersive x-ray powder diffraction (EDXRPD) data were obtained on station 9.7 at the Synchrotron Radiation Source (SERC Daresbury Laboratory). Samples were loaded in a similar manner as for the spectroscopic measurements, except NaCl was added instead of ruby as a pressure calibrant for most runs. An acquisition time of 1000 s was used.

III. RESULTS

A. Sodium hydrosulfide

NaSH was found to undergo two phase transitions upon compression. The first, an order-disorder transition, occurs below 9 kbar. The only spectroscopic change observed was the appearance of a shoulder on the infrared active S-H stretch, Table I and Figs. 2 and 3. The lattice modes were too weak to be observed in the DAC. The positions of the main band and shoulder at 20 kbar are almost identical to those of the corresponding Raman bands at 113 K,[14] indicating that it is probably phase III. The presence of two S-H stretches in either the IR or Raman spectrum of this phase is at odds with the structure as determined by neutron diffraction,[7] for which only one IR-active b_u and one Raman-active a_g mode would be expected. The IR and Raman bands of this phase are noncoincident within experimental error, and therefore the actual unit-cell size must be double that determined previously.

The second phase transition was observed beginning at 83 kbar. A new band appeared at more than 50 cm^{-1} below the phase-III band in both the IR and Raman spectra. This band gradually increased in intensity at the expense of the phase-III band; however, there was still a trace of phase III present at 209 kbar, Figs. 2 and 3. The high-pressure phase, phase-IV band was broader than the phase-III band and exhibited a negative pressure shift, Table I. These observations and the decrease in frequency at the phase transition indicate that hydrogen bonds are formed. The magnitude of this negative pressure shift is much smaller than that observed for strongly hydrogen-bonded materials, but is very similar to those observed in situations where a hydrogen atom is hydrogen bonded to more than one electronegative atom, such as in $Mg(OH)_2$ (Ref. 11) and LiOD.[5] It is therefore likely

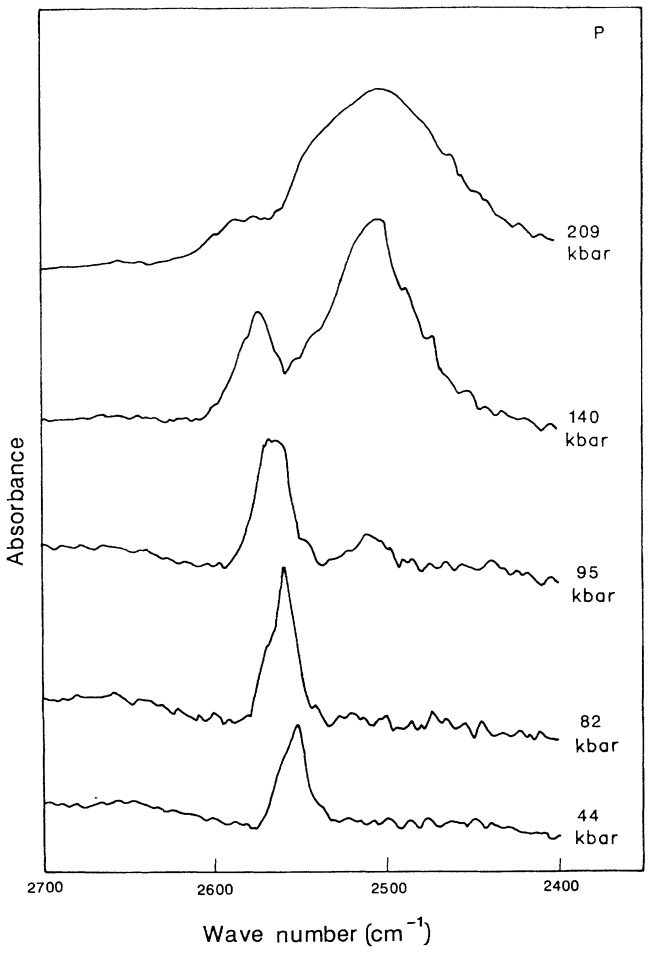

FIG. 2. IR spectrum of NaSH at various pressures.

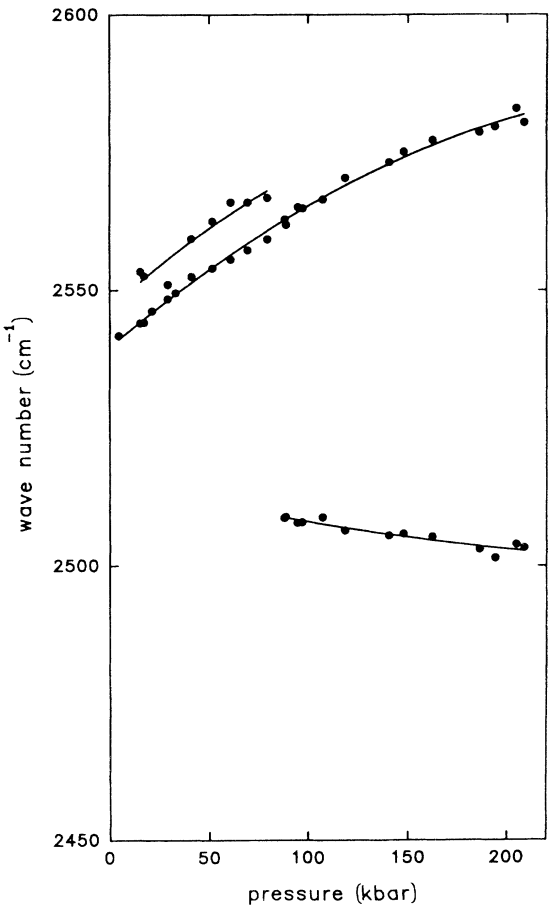

FIG. 3. Pressure dependence of the IR-active ν_{SH} in NaSH.

TABLE I. Raman and infrared data for NaSH.

Phase III (51 kbar)				Phase IV (107 kbar)				
ν_R cm^{-1}	ν_{IR} cm^{-1}	$d\nu/dp$ cm^{-1}/kbar	ν_0 cm^{-1}	ν_R cm^{-1}	ν_{IR} cm^{-1}	$d\nu/dp$ cm^{-1}/kbar	ν_0 cm^{-1}	Assignment
2559*m*		0.34	2542		2509*m*	−0.05	2513	ν_{SH}
	2563*sh*	0.34	2547	2500*m*		−0.15	2517	
	2554*m*	0.30	2539					

that the SH^- ions form bifurcated H bonds.

A large hysteresis was observed with the reverse transition beginning at below 35 kbar. This hysteresis and the large pressure range of intergrowth in both directions indicate that the transition involves an increase in sodium coordination in addition to the formation of hydrogen bonds.

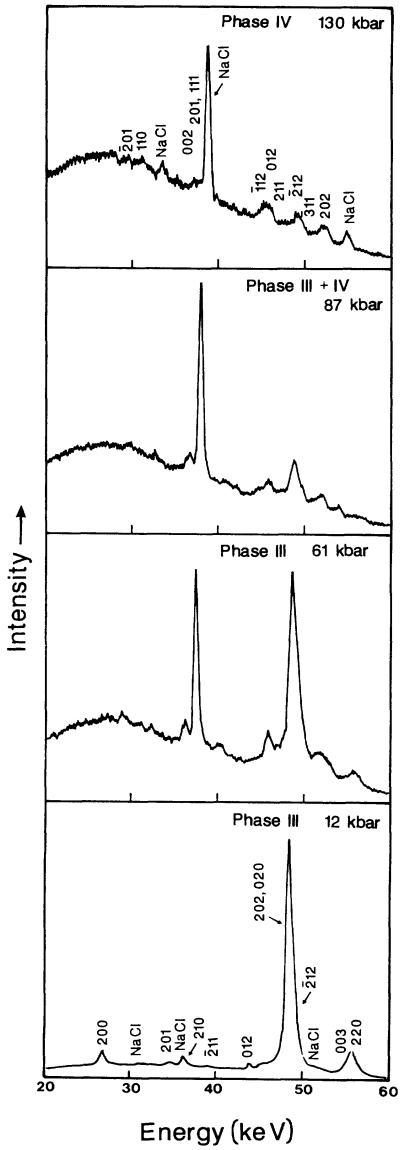

FIG. 4. EDXRPD patterns for NaSH with NaCl pressure calibrant (2θ=7.085°) (not to scale).

EDXRPD patterns for NaSH are shown in Fig. 4. No data were obtained from the ambient pressure phase. Data from the intermediate pressure phase indexed on a monoclinic cell, Table II, with the following cell constants at 12 kbar: a=7.502(26) Å, b=4.133(9) Å, c=5.552(20) Å, β=97.78(31)°, Z=4. This cell is equivalent to that of phase III at low temperatures,[7] except that it is doubled along **a** and the cell dimensions are reduced. The space group was chosen to be $P2_1/a$ as the vibrational data indicated that both this cell and the low-temperature cell must be double that determined previously. The ordered hydrogen positions are not known, but they would not be expected to deviate greatly from those determined at low temperature, except that in both cases they would be required to be canted slightly from their positions on the mirror plane, such that the mirror plane becomes a glide plane doubling the cell along **a**. This would be consistent with the small splitting in ν_{SH}. Major changes in the EDXRPD pattern were observed above the III-to-IV phase transition pressure. The pattern at 87 kbar still contained reflexions from phase III, but at 130 kbar the reflexions were almost exclusively from phase IV. Using a structural model, based on TII, the data could be indexed on a monoclinic cell with a=7.362(60) Å, b=3.698(8) Å, c=5.615(50) Å, β=104.50(51)°, Z=4 at 130 kbar, Table III. This corresponds to a structure in which the sulfur atoms are all in

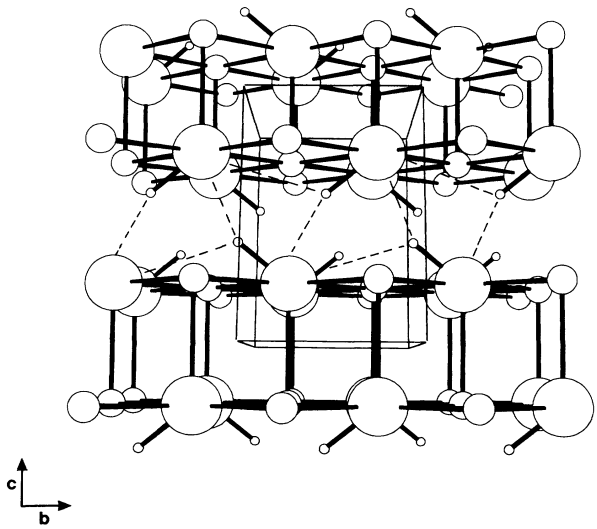

FIG. 5. Model structure for NaSH IV: circles represent S (large), Na (medium), and H (small); dashed lines show the hydrogen bonds belonging to one chain.

TABLE II. High-pressure EDXRPD data for NaSH III: $a=7.502(26)$ Å, $b=4.133(9)$ Å, $c=5.552(20)$ Å, $\beta=97.78(31)°$, $Z=4$ at 12 kbar.

d_{obs} (Å)	d_{calc} (Å)	$100\Delta d/d$	hkl
3.724	3.714	0.27	200
2.898	2.896	0.08	201
2.758	2.763	0.18	210
2.579	2.572	0.27	$\bar{2}11$
2.280	2.280	0.00	012
2.072	2.072	0.00	202
	2.065	0.34	020
2.047	2.049	0.10	$\bar{2}12$
1.799	1.805	0.33	220

TABLE III. High-pressure EDXRPD data for NaSH IV: $a=7.362(60)$ Å, $b=3.698(38)$ Å, $c=5.615(50)$ Å, $\beta=104.50(51)°$, $Z=4$ at 130 kbar.

d_{obs} (Å)	d_{calc} (Å)	$100\Delta d/d$	hkl
3.399	3.394	0.15	$\bar{2}01$
3.233	3.281	1.46	110
2.689	2.686	0.11	201
	2.676	0.49	111
2.245	2.222	1.04	$\bar{1}12$
2.187	2.189	0.09	012
	2.173	0.64	211
2.044	2.060	0.78	$\bar{2}12$
2.022	2.018	0.20	$\bar{3}11$
1.928	1.939	0.57	202

contact with one another. The space group would be $P2_1/a$ with bifurcated hydrogen-bonded chains running along **b**, Fig. 5.

B. Potassium hydrosulfide

Two phase transitions were detected in KSH on compression at 19 and 23 kbar, respectively. At the first transition, a decrease of more than 20 cm^{-1} in the IR- and Raman-active S-H stretches was observed, Figs. 6 and 7 and Table IV; however, these vibrations continued to harden in the intermediate pressure phase, phase IV, suggesting the absence of hydrogen bonds. It was very easy to overshoot this phase and, in order to obtain significant amounts of phase IV, samples had to be held at 20 kbar for 3 days. Alternatively, phase IV could be obtained at pressures between 15 and 20 kbar from the high-pressure phase, phase V.

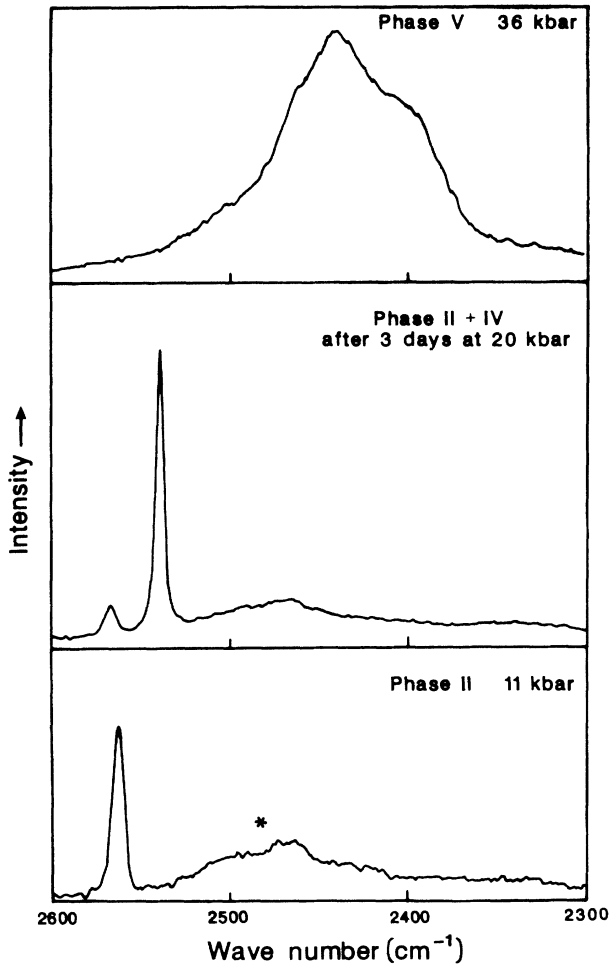

FIG. 6. Raman spectrum of KSH at various pressures (* represents the second-order diamond spectrum) (not to scale).

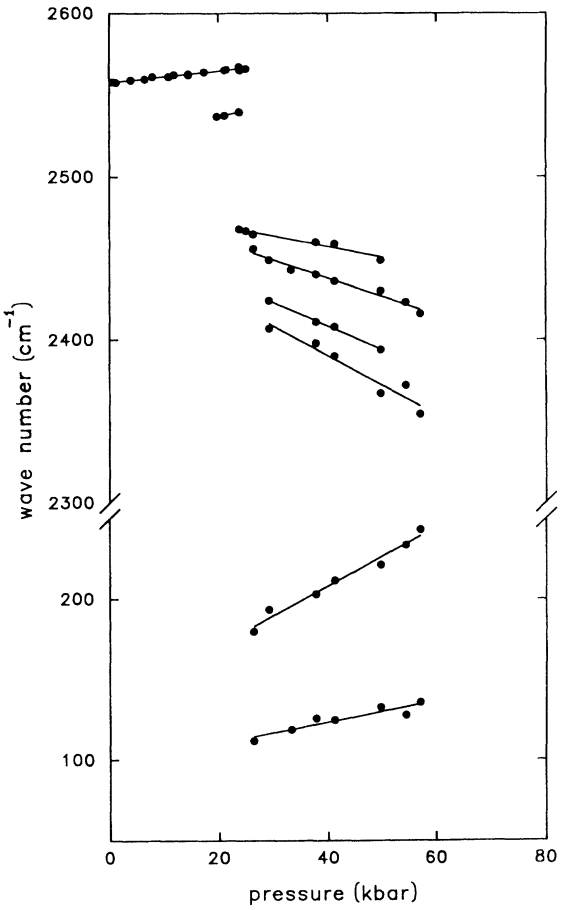

FIG. 7. Pressure dependence of the Raman-active modes of KSH.

TABLE IV. Raman and infrared data for KSH.

Phase II (8 kbar)				Phase IV (20 kbar)				Phase V (41 kbar)				
ν_R cm^{-1}	ν_{IR} cm^{-1}	$d\nu/dp$ cm^{-1}/kbar	ν_0 cm^{-1}	ν_R cm^{-1}	ν_{IR} cm^{-1}	$d\nu/dp$ cm^{-1}/kbar	ν_0 cm^{-1}	ν_R cm^{-1}	ν_{IR} cm^{-1}	$d\nu/dp$ cm^{-1}/kbar	ν_0 cm^{-1}	Assignment
									2640*m*	0.10	2637	ν_{SH}+lattice mode
2560*s*		0.35	2558	2538*s*		0.23	2533	2459*sh*		−0.61	2482	
	2557*m*	0.40	2553		2535*m*	0.18	2532	2436*vs*		−1.14	2483	
								2408*sh*		−1.44	2466	ν_{SH}
								2390*sh*		−2.10	2474	
									2428*vs*	−1.25	2482	
									2315*sh*	0.03	2315	ν_{SH}−lattice mode
								~569*vw*				R_{SH}
								~487*vw*				
								212*w*		1.58	148	
								125*w*		0.58	103	lattice modes

A decrease of more than 70 cm^{-1} in the S-H stretching frequency and significant broadening in the infrared and Raman spectra indicated that hydrogen bonds were formed at the 23-kbar transition. The symmetric S-H stretch split into four overlapping components, requiring that $Z \geq 4$ in the new phase. The negative presure shifts observed for the S-H stretches in this phase are similar to those observed for H_2O, H_2S, and organic alcohols,[15–19] which is consistent with the presence of strong hydrogen bonds. The extrapolated ambient pressure values for the S-H stretches, ν_0, are similar to the values reported at low temperatures for the H-bonded phase of CsSH,[14] but are slightly lower in frequency as expected since the S-S distances would be shorter in KSH. In addition, twice as many S-H stretches are observed in the Raman spectrum of KSH indicating that the primitive unit cell must be double that of low-temperature CsSH.

The intensity in both the IR and Raman spectra increased by more than an order of magnitude, which is indicative of the electronic changes which occur upon formation of the hydrogen bonds. This intensity increase is much greater than that observed for NaSH and would be consistent with the much stronger hydrogen bonding present. Two weak lattice modes were observed in the Raman spectra of phase V, which hardened with increasing pressure. It is probable that these modes involve hydrogen-bond stretching in addition to translational or rotational contributions. In addition, two SH^- librations were observed at 569 and 487 cm^{-1}. These bands are significantly higher in frequency than the 388-cm^{-1} libration reported for phase III at 30 K,[7] since they will also have a hydrogen-bond stretching contribution.

Upon decompression, the reverse transitions began at 22.5 and close to 17 kbar, respectively, indicating the absence of any significant hysteresis in the 23-kbar transition and a slight hysteresis in the 19-kbar transition. The region of stability of phase IV is small, ranging from a minimum of 3 to a maximum of 8 kbars.

EDXRPD data on KSH are shown in Figs. 8 and 9. Those of the ambient phase are in agreement with the known rhombohedral structure. Phase IV was obtained by first increasing the pressure above that of the IV-to-V transition and then reducing it to 15 kbar. The data were

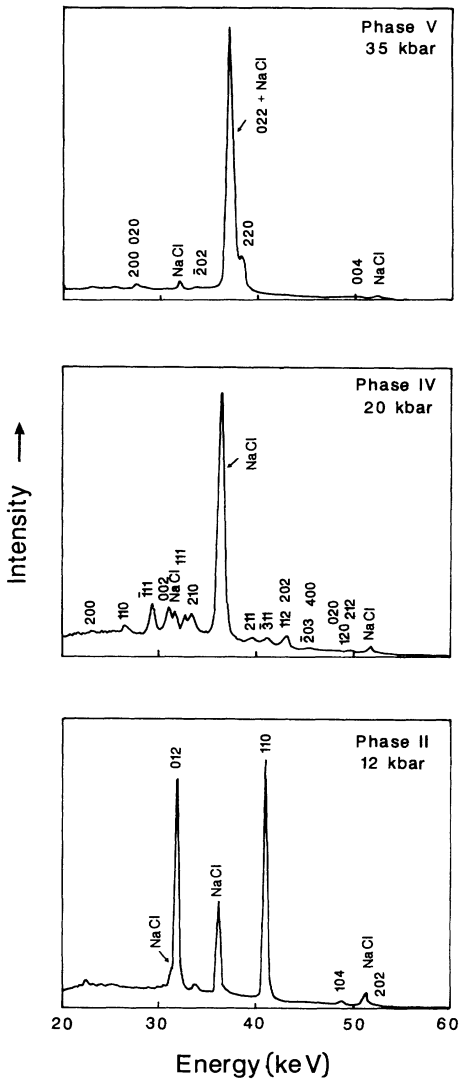

FIG. 8. EDXRPD patterns for KSH with a NaCl pressure calibrant ($2\theta = 7.067°$) (not to scale).

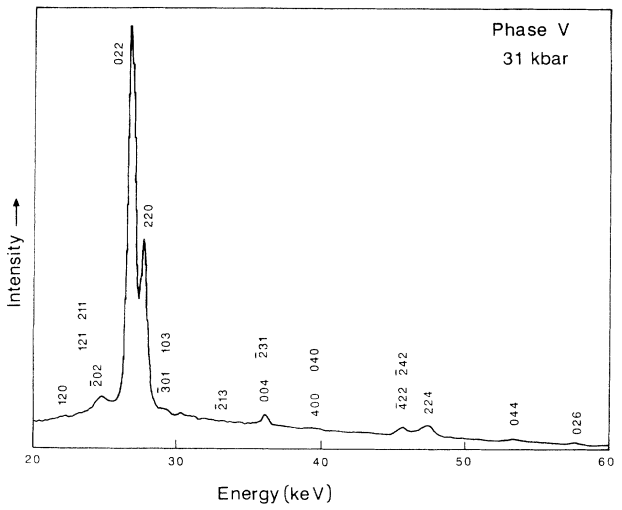

FIG. 9. EDXRPD pattern for KSH V with a ruby pressure calibrant ($2\theta = 9.819°$).

successfully indexed using a structural model based on a monoclinically distorted TlI structure with an assumed in-layer K-S distance of 3.09 Å. The refined cell constants were $a = 9.129(41)$ Å, $b = 4.181(18)$ Å, $c = 6.781(18)$ Å, $\beta = 106.47(27)°$, $Z = 4$ at 20 kbar, Table V. This corresponds to a structure with a $P2_1/a$ space group. The S-S distances between layers are 4.04 Å, which are short enough for hydrogen bonds to form, although this would be at odds with the positive dv/dp value for the S-H stretch. In addition, no splitting was observed for this mode, which indicates that dynamic disorder could persist. The disorder could involve jumps between equivalent positions along **b**, possibly involving the forming and breaking of weak hydrogen bonds. The evidence for cell doubling along **a** arises solely from the x-ray-diffraction data indicating that it could result from a distortion of the K-S sublattice.

Using a model based on a distorted CsCl structure, the data from phase V could be successfully indexed on a monoclinic cell with $Z = 1$. Weak superlattice reflexions, Fig. 9, and the spectroscopic data indicate that the actual unit cell is larger. The relative cell dimensions are very similar to those of the low-temperature phase of CsSD,[2] which has a tetragonally distorted CsCl structure, space group $I4/m$, $Z = 8$, suggesting that the structures are similar. In addition the relative intensities are qualitatively similar to the neutron-diffraction intensities for CsSD, with those of the superlattice peaks in the EDXRPD data being weaker than those in the neutron-diffraction data for CsSD. This would be expected as the ordered protons (deuterons) should contribute strongly to the intensity of the superlattice peaks in the neutron-diffraction pattern. The refined cell was found to have

TABLE V. High-pressure EDXRPD data for KSH IV: $a = 9.129(41)$ Å, $b = 4.181(18)$ Å, $c = 6.781(18)$ Å, $\beta = 106.47(27)°$, $Z = 4$ at 20 kbar.

d_{obs} (Å)	d_{calc} (Å)	$100\Delta d/d$	hkl
4.365	4.374	0.21	200
3.785	3.770	0.40	110
3.436	3.450	0.47	$\bar{1}11$
3.254	3.249	0.15	002
3.091	3.101	0.32	111
3.023	3.021	0.07	210
2.541	2.555	0.55	211
2.444	2.435	0.36	$\bar{3}11$
2.334	2.325	0.39	112
2.202	2.206	0.18	$\bar{2}03$
2.076	2.089	0.63	020
2.026	2.024	0.10	212

TABLE VI. High-pressure EDXRPD data for KSH V: $a = 7.448(22)$ Å, $b = 7.328(26)$ Å, $c = 8.110(22)$ Å, $\beta = 97.46(36)°$, $Z = 8$ at 31 kbar.

d_{obs} (Å)	d_{calc} (Å)	$100\Delta d/d$	hkl
3.278	3.280	0.07	120
2.937	2.933	0.14	211
	2.915	0.75	$\bar{2}02$
2.705	2.708	0.11	022
2.618	2.618	0.00	220
2.417	2.417	0.00	103
2.005	2.010	0.24	004
	2.009	0.20	$\bar{2}31$
1.842	1.846	0.22	400
	1.832	0.54	040
1.588	1.592	0.25	$\bar{4}22$
1.546	1.551	0.32	$\bar{2}42$
	1.542	0.26	332
1.526	1.531	0.33	105
	1.525	0.07	224
1.356	1.354	0.15	044, $\bar{4}24$
1.257	1.259	0.16	026

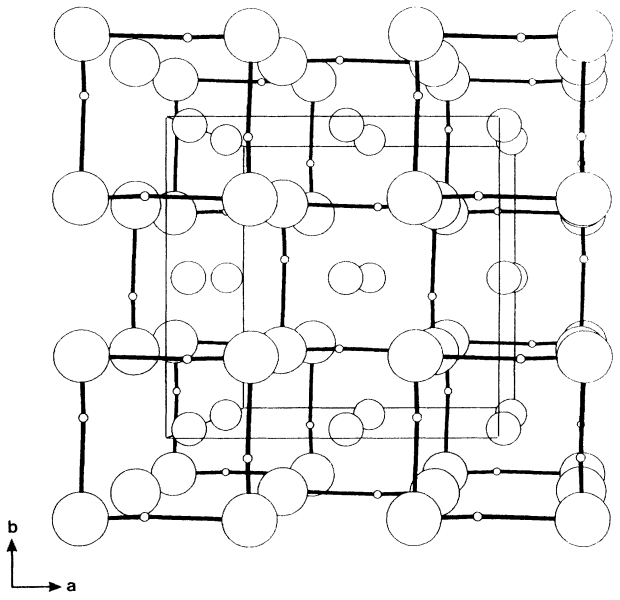

FIG. 10. Model structure for KSH V: circles represent S (large), K (medium), and H (small).

the following cell parameters at 31 kbar: $a=7.488(22)$ Å, $b=7.328(26)$ Å, $c=8.110(22)$ Å, $\beta=97.46(36)°$, $Z=8$, Table VI. This corresponds to a sheared version of the CsSD cell, proportionately reduced in size. If the proton ordering pattern is the same as that of CsSD with four-membered $S_4D_4^{4-}$ hydrogen-bonded units, then the shear along **a** will produce a triclinic structure with a $P\bar{1}$ space group, Fig. 10.

IV. DISCUSSION

The variation in cell constants and volume per formula unit for NaSH and KSH are shown in Figs. 11 and 12, respectively. In the case of NaSH, a volume change of 18.5% was observed between 0 and 9 kbar. This is a consequence of the disordered phase being highly compressible and the presence of an order-disorder transition in this pressure range. The corresponding volume change from the ambient to the low-temperature phase at 9 K in NaSD is 5.5%.[7] The additional decrease in volume at a high pressure of 13% is not unreasonable. The volume change at the 83-kbar transition is negligible, although the transition is reconstructive and corresponds to an increase in sodium coordination. This is a result of the ordered variant of the ambient phase already having a high density. The reconstructive nature of this transition accounts for the large hysteresis and pressure range of intergrowth observed. The uniaxial compressibilities, Table VII, indicate that the compressibility of both phases is highly anisotropic. In particular, in phase III, the cell is incompressible along **b**. In phase IV, the cell is incompressible except along **b**, which is the direction of the hydrogen-bonded chains. This might be expected as it corresponds to the longest S-S distance.

TABLE VII. Uniaxial and volume compressibilities and increase in β ($\times 10^3$ kbar) for NaSH.

Phase	a	b	c	β^a	V
III	1.1	0.0	0.7	0.3	1.8
IV	0.0	0.5	0.0	0.2	0.5

[a] $1/\beta_0 \partial\beta/\partial p$.

The ambient, disordered phase of KSH was found, as expected, to be highly compressible, Table VIII. Only a small volume change (1.0% at 19 kbar) and a slight reduction in compressiblity was observed at the III-to-IV transition, although there is an increase in potassium coordination from 6 to 7. This would be consistent with the persistence of dynamic disorder. A volume decrease

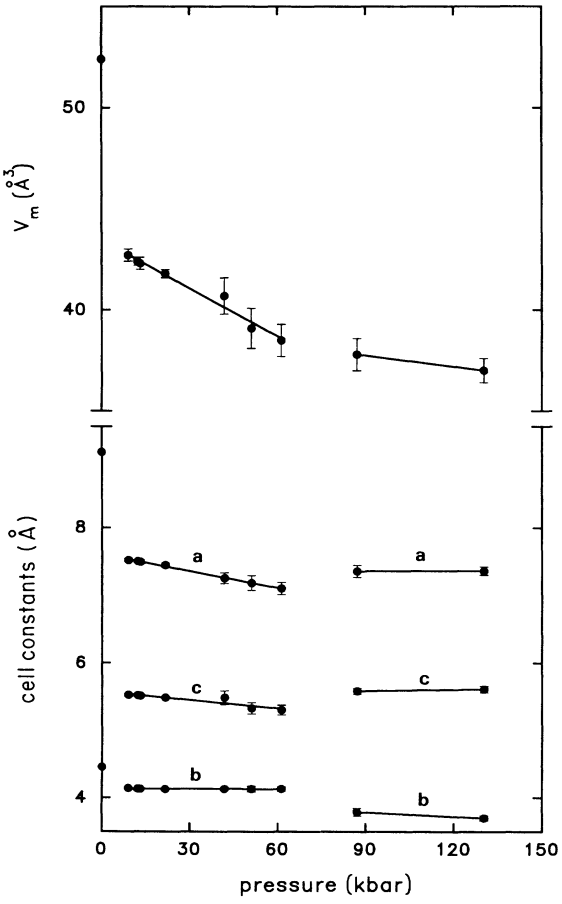

FIG. 11. Variation in cell constants and volume per formula unit with pressure for NaSH (ambient data are from Ref. 11).

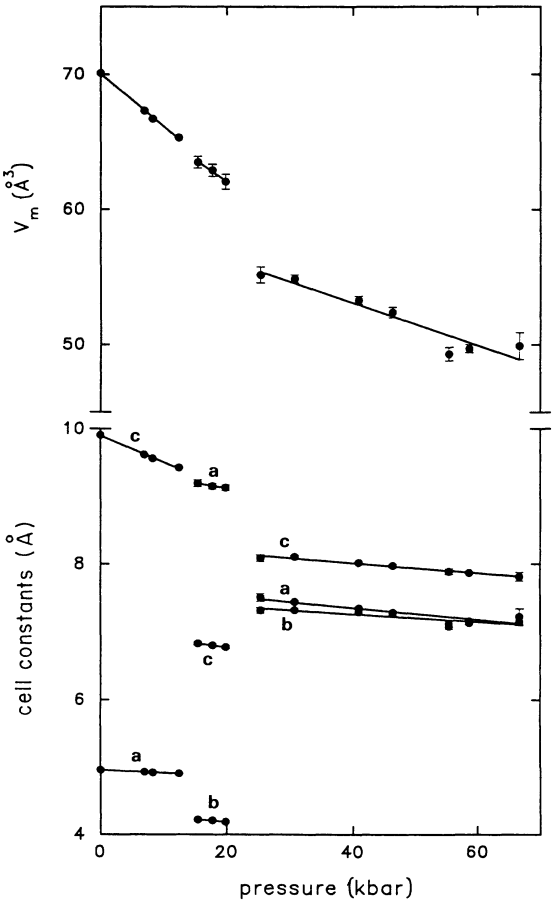

FIG. 12. Variation in cell constants and volume per formula unit with pressure for KSH (ambient data are from Ref. 8).

TABLE VIII. Uniaxial and volume compressibilities and increase in β ($\times 10^3$ kbar) for KSH.

Phase	a	b	c	β^a	V
II	0.8		4.0		5.6
IV	1.7	1.7	1.7	0.0	4.8
V	1.1	0.8	0.9	0.4	2.7

[a] $1/\beta_0 \partial\beta/\partial p$.

of 8.7% was observed at the 23-kbar transition corresponding to the increase in coordination number to 8, the formation of strong hydrogen bonds, and the bringing of the sulfur atoms into contact with one another.

The c direction in Phase II, along which the disordered SH^- ions lie, was found as expected to be highly compressible. KSH experienced close to isotropic compression in phase IV. This is not unreasonable, as based on the model, the S-S distances are all greater than 4 Å. In phase V, a was found to be more compressible than the other two directions. This results in the $S_4H_4^{4-}$ units gradually becoming square within experimental error above 40 kbar.

The transition pressures for NaSH and KSH are lower than those for the corresponding alkali halides, NaCl and KCl. This arises from the ability of the hydrosulfides to transform to a TlI-type structure, stablized by the nonspherical anions, rather than transforming directly to a CsCl-type structure. In the case of NaSH, contact between all neighboring sulfur atoms can be achieved in the TlI-type structure. This and the presence of hydrogen bonding results in it exhibiting a very large pressure range of stability, extending to over 209 kbar and delaying the onset of a hypothetical TlI-type–to–CsCl-type transition. The TlI-type phase in KSH, on the other hand, does not allow for sulfur-sulfur contacts, nor does it appear to be hydrogen bonded and it proceeds readily to a hydrogen-bonded CsCl-type phase with close S-S contacts at a similar pressure to that of the $B1$-to-$B2$ transition in KCl. The difference in behavior between the two hydrosulfides is a result of the difference in cation size.

It would appear from these and recent results that TlI-type structures are more common than previously believed. All the alkali-metal hydroxides,[4,5,20–23] NaSH and KSH, the group-IV chalcogenides, SnTe, PbS, PbSe, PbTe,[24] and NaBr and NaI (Ref. 25) adopt a TlI-type or a distorted TlI-type structure at high pressure or low temperature. In addition, GeS, GeSe, SnS, and SnSe adopt a distorted variant under ambient conditions.[26] This indicates that the TlI-type structure is the favored intermediate between the NaCl and CsCl types for systems with nonspherical atoms or ions. In fact, in situations where contact between all neighboring anions can occur in a TlI-type structure, this structure exhibits a very large range of stability.

For the alkali-metal hydrosulfides, it would appear that the type of structure adopted dictates the H-bonding scheme with chains of bifurcated H bonds for the TlI-type structure of NaSH and four-membered rings of near linear H bonds for the CsCl-type structure of KSH. Among the other hydrosulfides, LiSH could be expected to behave like NaSH and undergo a transition to a TlI-type structure as does LiOD,[4,5] while RbSH would adopt a high-pressure structure similar to that of KSH, but with a significantly lower transition pressure. In the cases of KSH, RbSH, and CsSH, there is strong potential for hydrogen-bond symmetrization of the type observed for H_2O (Refs. 27 and 28) and NH_3 (Ref. 29) at pressures in the order of 500 kbar. In the model structure for KSH at 31 kbar, the lengths of the S-H bond and the hydrogen bond are approximately 1.4 and 2.2 Å, respectively.

ACKNOWLEDGMENTS

We thank Dr. D. M. Adams (University of Leicester) for the use of his laboratory and for helpful suggestions and comments. We also thank S. M. Clark (SERC Daresbury Laboratory, U.K.) for assistance with the x-ray-diffraction experiments. This work was supported by SERC (U.K.). J.H. acknowledges support from the NSERC (Canada).

[1] T. J. Bastow, M. M. Elcombe, and C. J. Howard, Ferroelectrics **79**, 269 (1988).
[2] H. Jacobs and R. Kirchgässner, Z. Anorg. Allg. Chem. **569**, 117 (1989).
[3] D. M. Adams and J. Haines, J. Phys. Chem. **95**, 7064 (1991).
[4] D. M. Adams, A. G. Christy, and J. Haines, High Pressure Res. (to be published).
[5] D. M. Adams, A. G. Christy, and J. Haines, J. Phys. Chem. (to be published).
[6] D. M. Adams and J. Haines, J. Phys. Condens. Matter. **3**, 9503 (1991).
[7] H. Jacobs, U. Metzner, R. Kirchgässner, H. D. Lutz, and K. Beckenkamp, Z. Anorg. Allg. Chem. **598/599**, 175 (1991).
[8] H. Jacobs and C. Erten, Z. Anorg. Allg. Chem. **473**, 125 (1981).
[9] C. K. Coogan, G. G. Belford, and H. S. Gutowsky, J. Chem. Phys. **39**, 3061 (1963).
[10] K. R. Jeffrey, Can. J. Phys. **52**, 2370 (1974).
[11] L. W. Schroeder, L. A. de Graaf, and J. J. Rush, J. Chem. Phys. **55**, 5363 (1971).
[12] J. J. Rush, L. A. de Graaf, and R. C. Livingston, J. Chem. Phys. **58**, 3439 (1973).
[13] J. D. Barnett, S. Block, and G. J. Piermarini, Rev. Sci. Instrum. **44**, 1 (1973).
[14] J. J. Rush, R. C. Livingston, and G. J. Rosasco, Solid State Commun. **13**, 159 (1973).
[15] M. B. Kruger, Q. Williams, and R. Jeanloz, J. Chem. Phys. **91**, 5910 (1989).
[16] B. Minceva-Sukarova, W. F. Sherman, and G. R. Wilkinson, J. Phys. C **17**, 5833 (1984).
[17] H. Shimizu, Y. Nakamichi, and S. Sasaki, J. Chem. Phys. **95**, 2036 (1991).
[18] J. F. Mammone, S. K. Sharma, and M. Nicol, J. Phys. Chem. **84**, 3130 (1980).

[19]K. M. Yenice, M. D. Reed, S. A. Lee, and C. S. Chang, J. Raman Spectrosc. **22**, 679 (1991).
[20]T. J. Bastow, M. M. Elcombe, and C. J. Howard, Solid State Commun. **57**, 339 (1986).
[21]H. Jacobs, B. Mach, H.-D. Lutz, and J. Henning, Z. Anorg. Allg. Chem. **544**, 28 (1987).
[22]H. Jacobs, B. Mach, B. Harbrecht, H.-D. Lutz, and J. Henning, Z. Anorg. Allg. Chem. **544**, 55 (1987).
[23]B. Mach, H. Jacobs, and W. Schäfer, Z. Anorg. Allg. Chem. **553**, 187 (1987).
[24]T. Chattopadhyay, H. G. von Schnering, W. A. Grosshans, and W. B. Holzapfel, Physica B **139&140**, 356 (1986).
[25]T. Yagi, T. Suzuki, and S. Akimoto, J. Phys. Chem. Solids **44**, 135 (1983).
[26]H. Wiedemeier and H. G. von Schnering, Z. Kristallogr. **148**, 295 (1978).
[27]A. Polian and M. Grimsditch, Phys. Rev. Lett. **52**, 1312 (1984).
[28]K. R. Hirsch and W. B. Holzapfel, J. Chem. Phys. **84**, 2771 (1986).
[29]M. Gauthier, Ph. Pruzan, J. C. Chervin, and J. M. Besson, Phys. Rev. B **37**, 2102 (1988).